JASA ARTICLE

Using heat maps in teaching acoustics: Interaction of incident plane wave or incident beam with a solid plane structure[a)]

Catherine Potel,[1,b)] Philippe Gatignol,[2] and Michel Bruneau[1]

[1]*Laboratoire d'Acoustique de l'Université du Mans (LAUM), UMR 6613, Institut d'Acoustique—Graduate School (IA-GS), CNRS, Le Mans Université, Le Mans, 72085 Cedex 9, France*

[2]*Laboratoire Roberval, Université de Technologie de Compiègne, Alliance Sorbonne Université, FRE UTC/CNRS 2012, CS 60319, 60203 Compiègne Cedex, France*

ABSTRACT:

Using heat maps provides frame and relevance to topics covered in physical acoustics courses as students can more easily visualize complex ideas and situations. Students can also form a much better understanding of the physical phenomena involved and build more advanced critical thinking when heat maps are used. It is the aim of the paper to provide ways for students to interact with heat maps by using two examples: first, the interaction of a plane wave (not only monochromatic) with an interface separating a fluid and a solid medium and, second, the interaction of an acoustic beam with such an interface (including a solid layer). These heat maps permit both to describe non-specular effects for the reflected acoustic beam due to the generation of a modal wave and, in the case of anisotropic media, highlight the difference between the direction predicted by Snell-Descartes law and that predicted by energy flux. © *2022 Acoustical Society of America.*

https://doi.org/10.1121/10.0013013

(Received 12 November 2021; revised 6 July 2022; accepted 11 July 2022; published online 1 August 2022)

[Editor: Daniel A Russell] Pages: 754–764

I. INTRODUCTION

In many acoustic (among other fields) problems, it is very difficult to express all of the complexities of the physical phenomena by using only mathematical formulations of the problems and analytical methods for their resolution. Commonly used and very informative in research, plots of the spatial representation of acoustic fields are not well documented for teaching (to the authors' knowledge). More advanced insight is usually requested by every motivated student. In reality, to explain the essential features of the behavior of acoustic problems, detailed illustrations (pictures, graphics, heat maps, plots, etc.) may help the students to gain a deep insight into the role of fundamental physical laws and understand how the most important parameters affect the behavior. More particularly, using heat maps provides frame and relevance to topics covered in physical acoustics courses as students can more easily visualize complex ideas and situations (total reflection, interferences, far field, critical angles, etc.). Students can also form a much better understanding of the physical phenomena involved and can build more advanced critical thinking when heat maps are applied. The aim of the paper is twofold: first, to provide ways for students to interact with heat maps, which provide spatial representations of the phenomena involved, by using two examples presented in Secs. II and III; and, second, to describe (for the attention of fellow educators) how such heat maps could be used in a lesson using the authors' experience and give tips to reproduce some of them.

In Sec. II, the interaction of a plane wave (not only monochromatic) with an interface separating a fluid from a solid medium is discussed. The approach involves three kinds of incident waves: a rectangular wave (Sec. II A), a sine wave modulated by a shaped-like Gaussian function (Sec. II B), and a monochromatic wave (Sec. II C). Some examples of practical use are given in Sec. II D. In Sec. III, the interaction of a bidimensional incident Gaussian bounded beam with plane solid structures is presented. There are two main advantages of using heat maps to emphasize the phenomena involved. One advantage is to highlight the difference between the direction predicted by Snell-Descartes law and the direction of the energy flux in the case of anisotropic media (Sec. III B). The other advantage is to emphasize the non-specular reflection when a generalized modal wave is generated (Sec. III C). Note that pedagogically speaking, a back and forth between plane wave propagation and more or less directional beam propagation during courses permits us to establish a connection between the propagation direction of reflected and transmitted waves predicted by Snell-Descartes law and the direction propagation of energy. In the frame of the decomposition into plane waves, the Appendix provides some calculus and an algorithm and programming tips using matrix computation software for a fluid/fluid structure, which can be easily adapted in solid media.

[a)]This paper is part of a special issue on Education in Acoustics.

[b)]Electronic mail: catherine.potel@univ-lemans.fr

https://doi.org/10.1121/10.0013013

II. INTERACTION OF A PLANE WAVE WITH AN INTERFACE SEPARATING A SEMI-INFINITE FLUID AND A SEMI-INFINITE ISOTROPIC SOLID

Let

$$A = f(\xi), \tag{1a}$$

where

$$\xi = \frac{\mathbf{n}\cdot\mathbf{OM} - c_o t}{a} \tag{1b}$$

denotes the particle displacement amplitude of a plane wave propagating in a fluid medium at any given point, $M(x,z)$, O is the origin of a coordinate system, where a is the length scale of the signal, $\mathbf{n}$ is the propagation direction, and c_0 is the adiabatic speed of sound. We consider that this wave interacts with a plane interface located at $z = 0$, separating the fluid medium from an isotropic solid medium (Lamé coefficients λ and μ). So, it creates, classically, a longitudinal reflected wave and two transmitted waves [a pressure wave (P) and a shear vertical wave (SV)], whose propagation directions can be predicted by Snell-Descartes law. The aim of this section is to gradually show to the students how the shape of the function, f, affects the acoustic field while the critical angles (measured from the normal to the interface) and the reflection and transmission coefficients remain the same in each case. Here, for brevity, the case of incident angles greater than the first critical angle is considered only for monochromatic plane waves. It should be noted that all of this section can either precede or follow a full academic presentation (basic equations and their analytical solutions, results, and discussions), depending on whether the students are receptive or not to a mathematical presentation.

A. Rectangular incident signal

The advantage in first using a rectangular incident signal (see Fig. 1),

$$f(\xi) = \mathrm{rect}(\xi), \tag{2}$$

is that due to the finite spatial width of the signal, the different waves are clearly separated. There is just a "mixing" zone for approximatively $|x/a| \le 4$ and $-1 \le z/a \le 4$, but it is possible to clearly identify the transmitted P- and SV-waves and see that the rays predicted by Snell-Descartes law [black lines in Fig. 1(b)] are perpendicular to the wave planes.[1–3] It is also interesting to notice that the width of the transmitted signal depends on the speeds of sound in each medium and the boundary conditions are satisfied at the interface at $z = 0$.

B. Sine modulated by a shaped-like Gaussian function

Then, an incident signal of the form

$$f(\xi) = \cos(ka\xi)/\left(1+\xi^2\right), \tag{3}$$

where k (m^{-1}), analogous to a wave number corresponding to a "local" wavelength λ with $a \gg \lambda$, presents the advantage to be similar to a more realistic signal, like a "burst." As the amplitude of the signal tends to zero when ξ tends to $\pm\infty$, it is also possible to well separate, relatively, the incident from the reflected plane waves (see Fig. 2 for $|x/a| \ge 10$). However, the total field in the fluid medium, which is the sum of the incident and reflected fields, presents some interference pattern forms which can be seen when $|x/a| \le 5$. These pattern forms prefigure those which appear in the whole fluid domain when the plane wave is monochromatic (Fig. 3). It is interesting to show to the students that the total transmitted field of Fig. 2(c) is the summation of the longitudinal (pressure) field [Fig. 2(a)] and the shear vertical field [Fig. 2(b)].

C. Monochromatic incident wave

Finally, when the incident wave is of the form

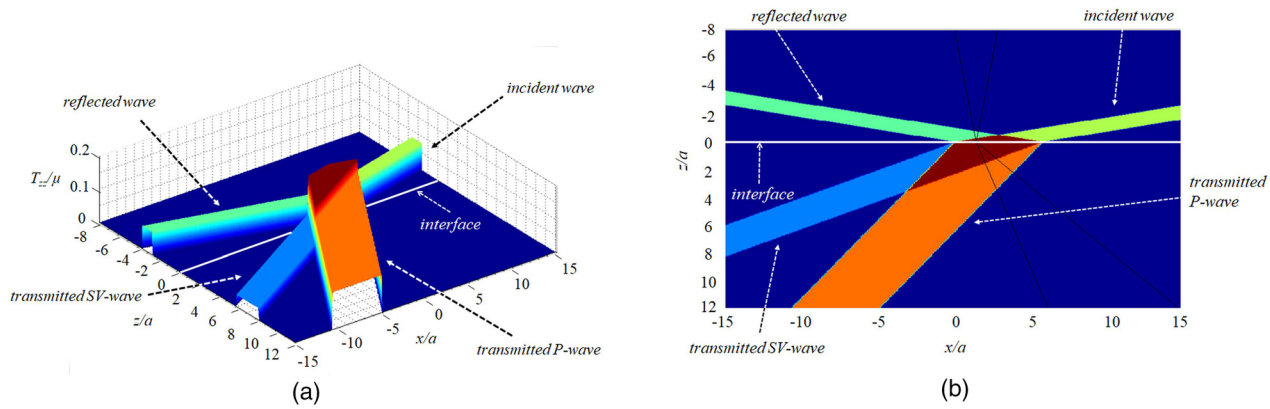

FIG. 1. (Color online) Snapshot at a given time, t, of the normalized normal stress, T_{zz}/μ, in the plane, (x,z), perpendicular to the interface plane, (x,y), when a rectangular plane wave [see Eq. (2)] propagating in a fluid medium interacts with an interface between the fluid medium and an isotropic solid medium, located at $z/a = 0$ (μ is the second Lamé coefficient). The incident angle is smaller than that of the first critical angle. The (a) three-dimensional (3D) representation and (b) top view of Fig. 1(a) are shown. The black lines represent the incident, reflected, and transmitted propagation directions, such as was predicted by Snell-Descartes law.

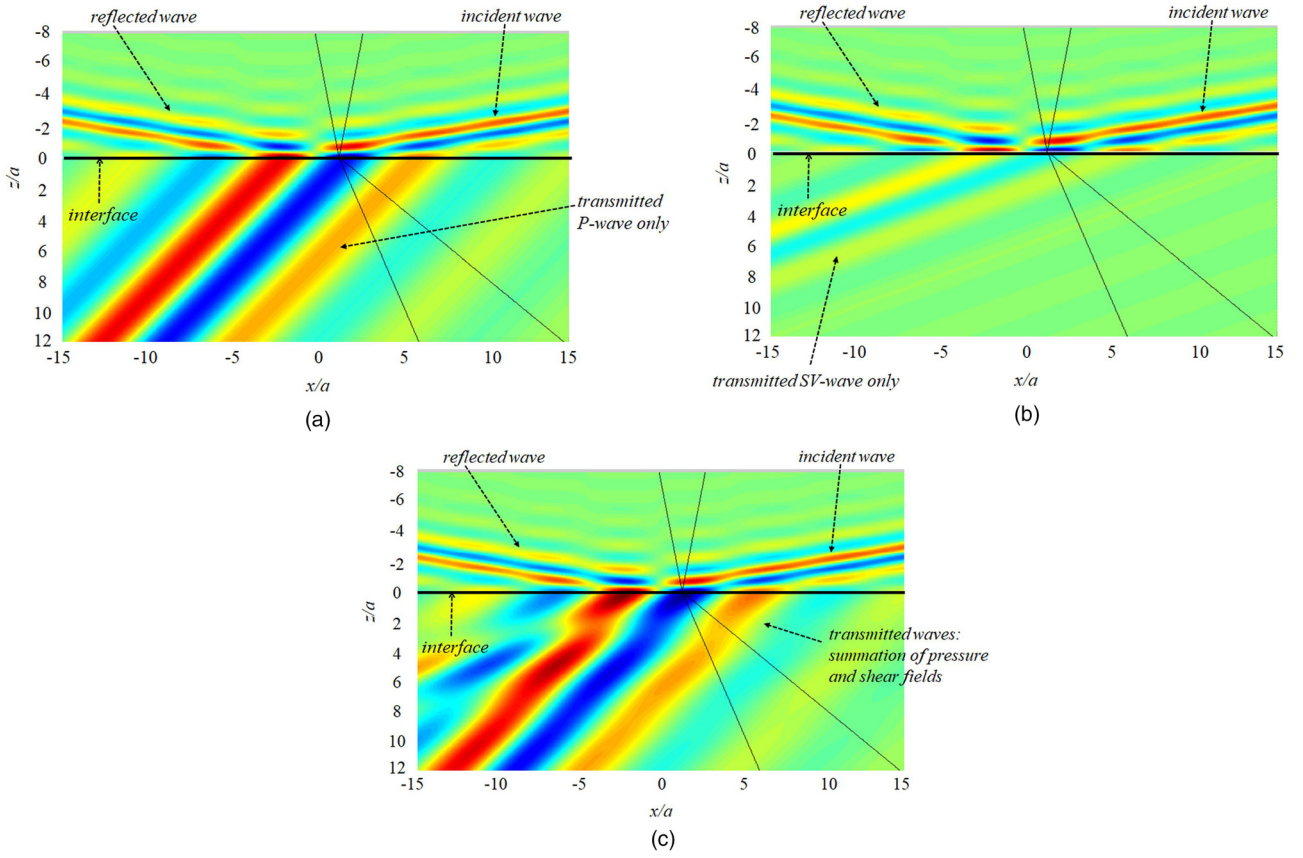

FIG. 2. (Color online) Snapshot at a given time, t, of the normalized normal stress, T_{zz}/μ, in the plane, (x, z), perpendicular to the interface plane, (x, y), when a sine modulated by a Gaussian-like function [see Eq. (3)] propagating in a fluid medium interacts with an interface between the fluid medium and an isotropic solid medium, located at $z/a = 0$. The incident angle is less than to the first critical angle. The black lines represent the incident, reflected, and transmitted propagation directions, such as was predicted by Snell-Descartes law. (a) Only the transmitted pressure wave field in the isotropic solid medium, (b) only the shear wave field in the isotropic solid medium, and (c) the sum of the pressure field and shear field are shown.

$$f(\xi) = \cos(ka\xi), \tag{4}$$

it is interesting to observe the interference fringes in overlapping incident and reflected fields in Fig. 3: the interference pattern forms of Fig. 2 are now present in the whole fluid medium.

When the incident angle is comprised between the two critical angles, the P-wave is evanescent in the isotropic solid medium [Fig. 4(a)]. Even if the propagative transmitted field is globally a SV field, there is still a small region in the vicinity of the interface which presents a small perturbation due to the evanescent wave. When the incident angle is greater than the second critical angle, the exponential decreasing form of the acoustic field can easily be observed in Fig. 4(b).

D. Practical use in class

Generally speaking, students struggle to have a spatial mental representation of an acoustic field, and although they are very familiar with using plane waves (often mainly monochromatic plane waves), they find it difficult to view them. The authors find it very useful to start by folding a sheet of A4 paper into a crenel shape and moving it around the classroom to simulate the interaction of a non-monochromatic plane wave with an interface. After drawing a horizontal line on the blackboard (simulating a plane interface), placing this sheet of paper on the blackboard permits us to simulate the incident wave, reflected wave, and transmitted wave and, thus, makes it possible to understand what Fig. 1(a) represents.

The practical use of the above-described heat maps in the classroom (according to the experience of the authors) depends on the academic level of the students and the purpose of their training.

- Undergraduate students preparing for a vocational degree, which does not require high mathematical skills, usually focus their interests and goals on applied studies. Therefore, first, one can ask the students what are, in their opinion, the phenomena involved in the interaction of a plane wave with an interface separating two semi-infinite media (fluid or solid). Second, to answer their questions and further introduce the physical phenomena, it is very useful to use (i) the slowness curves (see Sec. III B) to make it possible to comprehend the notion of critical angles and (ii) the heat maps to visualize the physical phenomena. Pedagogically speaking, the gradual transition from a non-monochromatic plane wave to a monochromatic plane wave has the advantage of preparing the interference pattern form, which can be seen in Figs. 2–4.

https://doi.org/10.1121/10.0013013

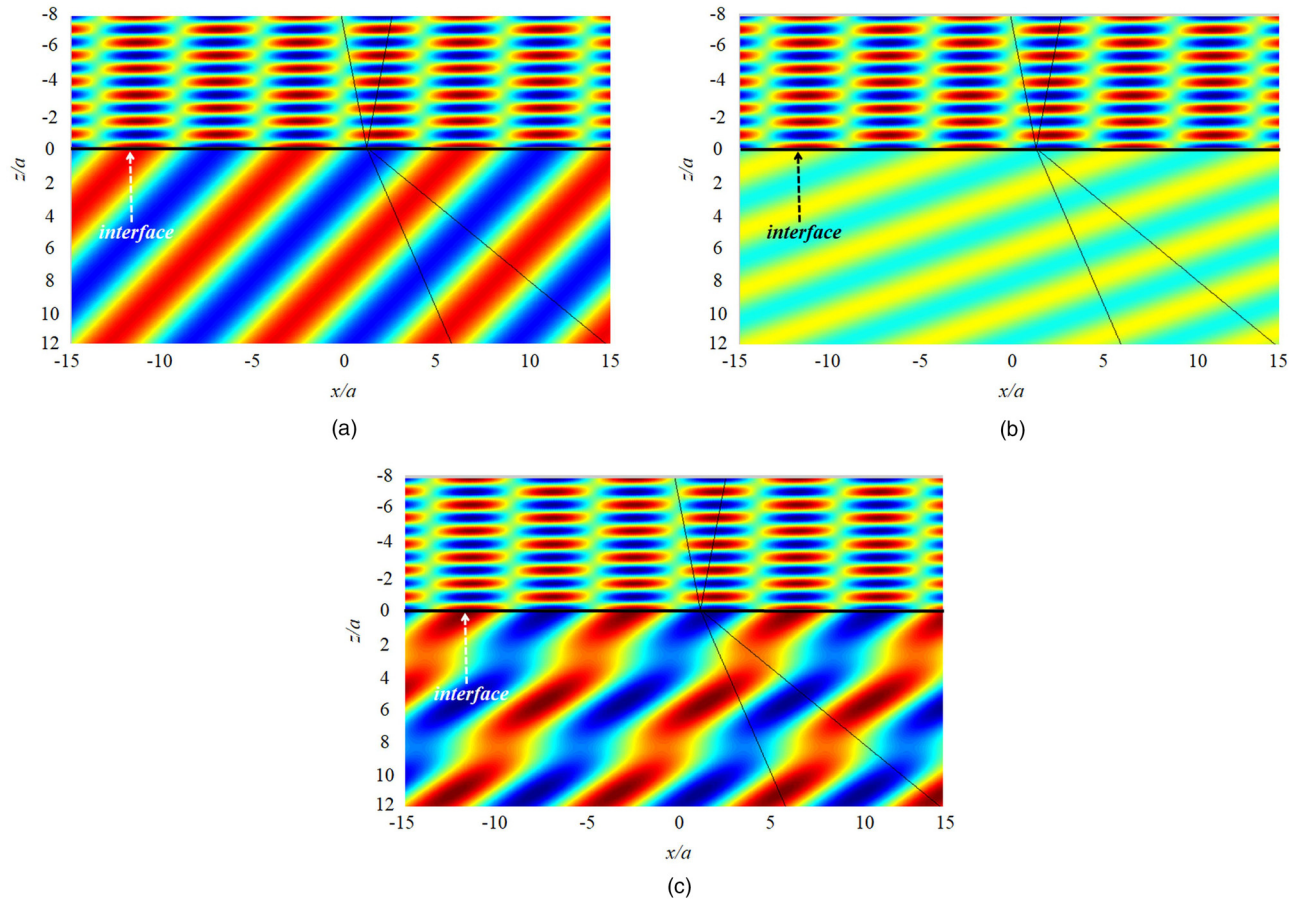

FIG. 3. (Color online) Snapshot at a given time, t, of the normalized normal stress, T_{zz}/μ, in the plane, (x, z), perpendicular to the interface plane, (x, y), when a monochromatic plane wave [see Eq. (4)] propagating in a fluid medium interacts with an interface between the fluid medium and an isotropic solid medium located at $z/a = 0$. The incident angle is smaller than the first critical angle. The black lines represent the incident, reflected, and transmitted propagation directions, such as was predicted by Snell-Descartes law. (a) Only the transmitted pressure wave field in the isotropic solid medium, (b) only the shear wave field in the isotropic solid medium, and (c) the sum of the pressure field and shear field are shown.

- On the other hand, undergraduate students who intend to undertake a master's degree are able and willing to carry out to the end a number of mathematical calculations, and depending on their state of tiredness or motivation, which any teacher can perceive when teaching, showing the heat maps in the middle of somewhat difficult calculations helps to re-motivate them. They generally ask many questions and, finally, link together physical

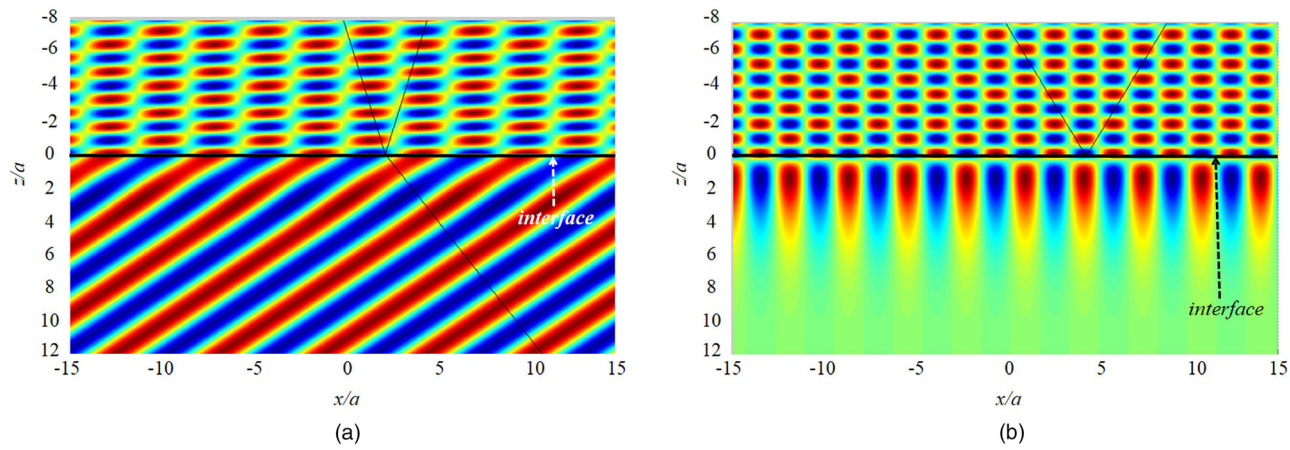

FIG. 4. (Color online) Snapshot at a given time, t, of the normalized normal stress, T_{zz}/μ, in the plane, (x, z), perpendicular to the interface plane, (x, y), when a monochromatic plane wave [see Eq. (4)] propagating in a fluid medium interacts with an interface between the fluid medium and an isotropic solid medium located at $z/a = 0$. (a) The incident angle is comprised between the two critical angles. (b) The incident angle is greater than that of the second critical angle.

phenomena and acoustic field calculations. In addition to these seminars, numerical practical works can be offered, which allow students to vary themselves with the parameters of an experiment. They do not plot the heat maps of Figs. 1–4, but they use part of research software which allows them to draw reflection and transmission coefficients for displacement amplitude and energy, for any structure, namely, medium 1/medium 2 or medium 1/medium 2/medium 3. These coefficients can be plotted as a function of the incident angle and/or the frequency of the incident wave. Time signals can also be plotted. Students can choose different material properties, different thicknesses, different types of incident waves, etc., and then they can explain, physically, why such reflection and transmission coefficients correspond to such types of waves, can detect echoes, and can interpret both in terms of nondestructive testing (NDT) and several types of waves (Lamb waves, etc.).

III. INTERACTION OF AN INCIDENT GAUSSIAN BOUNDED BEAM WITH PLANE SOLID STRUCTURE

Even if the case of a plane wave is very educative in the learning process of students, it is also interesting to show them some more realistic situations involving acoustic bounded beams to simulate the acoustic field produced by a transducer (diameter denoted $2a$). This is an opportunity to show them simulations closer to a real situation other than the one using plane waves and talk about NDT, emphasizing the need to know the characteristics of the materials used, the critical angles, etc., to comprehend how to conduct an experiment. The model chosen here is bidimensional. The incident beam is decomposed into monochromatic plane waves through a Fourier representation of the field[4–13] (in the Appendix, see the basic equations and some tips compute the different fields using matrix computation software). The emitting transducer is modelized by a vibrating plane immersed in a fluid medium (see Fig. 12 in the

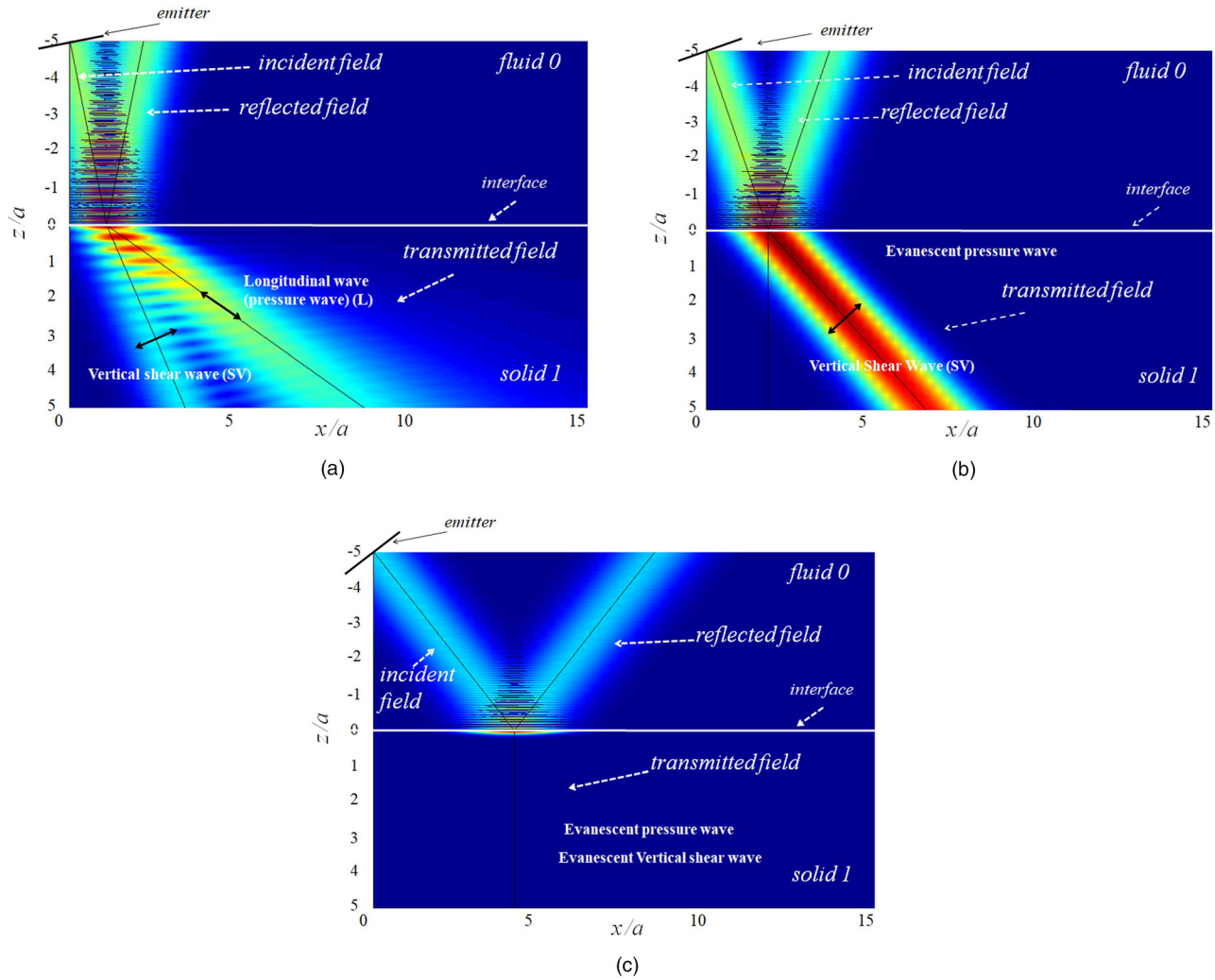

FIG. 5. (Color online) Heat map of the modulus of the stress vector for an incident monochromatic Gaussian bounded beam propagating in a fluid medium ($k_0a = 60$), which interacts with an interface between the fluid medium and an isotropic solid medium, located at $z/a = 0$. The emitting transducer is situated in the upper left angle of the figures ($x/a = 0, z/a = -5$). The black lines represent the incident acoustic axis of the emitter transducer and the reflected and transmitted propagation directions, such as was predicted by Snell-Descartes law. The incident angle is (a) smaller than the first critical angle, (b) comprised between the two critical angles, and (c) greater than the second critical angle.

https://doi.org/10.1121/10.0013013

Appendix). It is excited by a monochromatic signal such that the vibration amplitude is a Gaussian function, $\exp(-x_e^2/a^2)$, of the coordinate x_e on the plane emitter. To obtain a well collimated beam, the characteristic product k_0a (where $k_0 = \omega/c_0$) is chosen relatively high ($k_0a \geq 60$ in the following examples), but an example is given in Fig. 13 in the Appendix for a lower k_0a.

A. Case of an interface between semi-infinite fluid medium and semi-infinite isotropic solid medium

The choice of $k_0a = 60$ permits us to obtain several acoustic beams centered on the directions predicted by Snell-Descartes law (see Fig. 5). When the incident angle of the acoustic axis of the incident beam is greater than the critical angles [Fig. 5(c)], all of the transmitted waves are evanescent, and it is worthwhile to make the students notice that even if the acoustic field is mostly null in the solid, there is a small region in the vicinity of the interface where the stress is nonzero due to the fact that the boundary conditions must be fulfilled. Note that the black double-headed arrows in Fig. 5(a) are just there to remind the students that for the longitudinal wave, the particles vibrate in a direction parallel to the propagation direction vector, and for the shear wave, they vibrate in a direction perpendicular to the propagation direction vector.

B. Case of an interface between semi-infinite fluid medium and semi-infinite anisotropic solid medium

When an anisotropic solid medium is involved, it is very useful to draw the slowness surfaces given by the ends of the slowness vector of each wave propagating in the medium

$$\mathbf{m} = \mathbf{n}/V, \tag{5}$$

where V is the speed of each wave, drawn from a fixed point, O. Figure 6 shows the intersection of the slowness surfaces with the plane (Oxy) for an unidirectional composite medium for which the A6-axis is perpendicular to an interface fluid/solid [i.e., the solid is transversally isotropic, the isotropic plane is the plane (Oxy) of the interface]. In anisotropic media, the propagation direction does not generally coincide with the direction of the energy velocity.[1–3,14] This last direction can be easily deduced graphically by the use of the slowness curves: at a given incident angle (which corresponds to a given projection, m_x, of the slowness vector, $\mathbf{m}$, onto the interface, materialized by the intersection between a dotted vertical line and the x axis), the direction of the energy propagation, i.e., of the group velocity, is perpendicular to the tangent of the slowness curves at the intersection between the curves and the vertical line (see the small blue arrows in Fig. 6). It is particularly useful for the students to combine these properties with the heat map of Fig. 7: the transmitted bounded beams of the quasi-longitudinal waves and quasi-shear vertical waves are centered on the white lines corresponding to the direction of the energy velocity and not on the black lines corresponding to the propagation directions predicted by Snell-Descartes law. It should be noted that due to the symmetries, shear horizontal (SH) waves do not propagate.

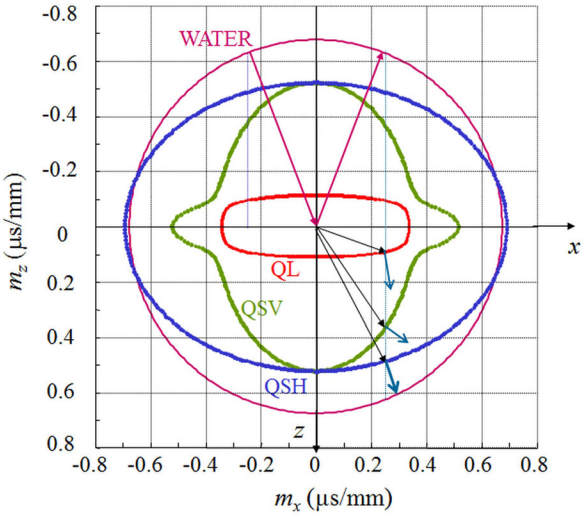

FIG. 6. (Color online) Slowness curves of water and an anisotropic solid medium (unidirectional carbon-epoxy medium, A6-axis perpendicular to the interface). For a projection, $m_x = 0.25$ μs mm^{-1}, of the slowness vector onto the interface, the small blue arrows show the direction of the energy velocities of the quasi-longitudinal (QL), quasi-shear vertical (QSV), and quasi-shear horizontal (QSH) waves.

C. Case of generalized modal waves

The aim of this section is to show the interest of the heat maps in the case of the generation of modal waves,[15] such as surface waves and guided waves, by the incident beam. For a given incident angle of the acoustic axis of the transducer and (in the case of Lamb waves) its main frequency, there is a progressive re-emission in the incident

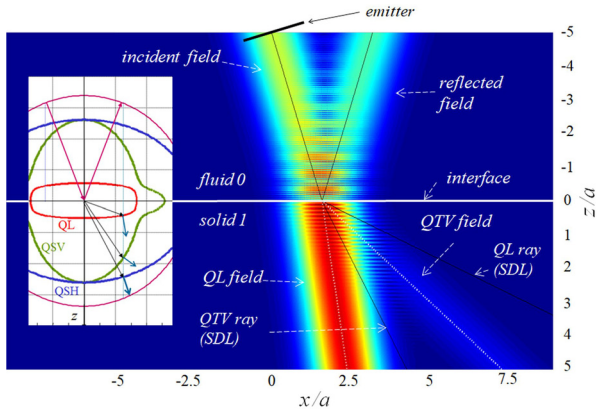

FIG. 7. (Color online) Heat map of the modulus of the stress vector for an incident monochromatic Gaussian bounded beam propagating in water ($k_0a = 170$), which interacts with an interface between the fluid medium and an anisotropic solid medium, located at $z/a = 0$ (unidirectional carbon-epoxy medium, A6-axis perpendicular to the interface, incident angle equal to 21.7°; see Fig. 6). The emitting transducer is situated at $(x/a = 0, z/a = -5)$. The black lines represent the incident acoustic axis of the emitter transducer, the reflected, and transmitted propagation directions, such as was predicted by Snell-Descartes law (SDL). The white lines in the solid represent the direction of the energy velocity.

medium of the energy conveyed by the modal wave: this phenomenon is well known as "leaky waves." Therefore, the reflected wave may appear as slightly translated with respect to the impact zone, and a "null zone" may appear due to the fact that the specular reflected beam and the leaky wave are out of phase.

1. Generalized Rayleigh waves

When the incident angle of the acoustic axis of an incident bounded beam propagating in a fluid corresponds to the propagation of a Rayleigh wave in the solid, it is well known that there is a radiation of the Rayleigh beam field in the fluid with a null reflection and a non-specular reflection.[1–3] These fields can be easily observed in Fig. 8, together with the surface wave.

2. Generalized Lamb waves

In the same way, when the incident angle of the acoustic axis of an incident bounded beam propagating in a fluid corresponds to the propagation of a Lamb wave in an isotropic layer immersed in the fluid, it is also well known that there is a radiation of the Lamb beam field in the fluid with a null reflection and a non-specular reflection (and non-specular transmission).[12,16] These fields can be easily observed in Fig. 9, together with the guided wave.

IV. CONCLUSION

To conclude, an attempt was made to show how the use of heat maps may help, profoundly, to convey interpretations of the physical phenomena and give the role played by parameters. Thus, making links between mathematical formulations and their physical meaning and visualizing complex situations, students can build more advanced critical thinking. Specifically, we have shown that it is very useful,

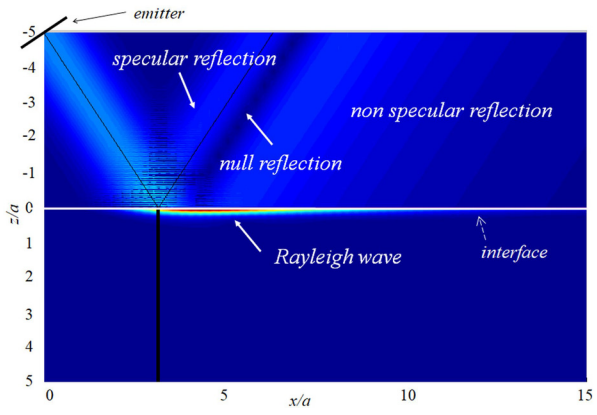

FIG. 8. (Color online) Heat map of the modulus of the stress vector for an incident monochromatic Gaussian bounded beam propagating in water ($k_0a = 60$), which interacts with an interface between the fluid medium and an isotropic solid medium, located at $z/a = 0$, for an incident angle corresponding to the propagation of a Rayleigh wave in the solid. The emitting transducer is situated at the upper left angle of the figure $(x/a = 0, z/a = -5)$. The black lines represent the incident acoustic axis of the emitting transducer, the reflected, and transmitted propagation directions, such as was predicted by Snell-Descartes law.

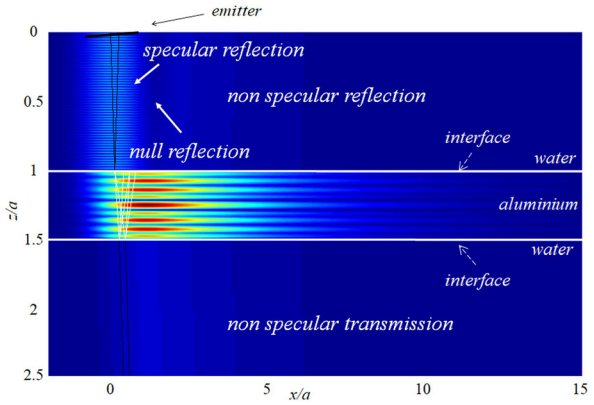

FIG. 9. (Color online) Heat map of the modulus of the stress vector for an incident monochromatic Gaussian bounded beam propagating in water ($k_0a = 170$), which interacts with an isotropic layer immersed in water (interfaces located at $z/a = 1$ and $z/a = 1.5$), for an incident angle corresponding to the propagation of a Lamb wave in the solid. The emitting transducer is situated at $(x/a = 0, z/a = 0)$. The white lines represent some reflections of the partial waves in the solid, corresponding to the incident acoustic axis of the emitting transducer, such as was predicted by Snell-Descartes law.

while teaching the propagation of acoustic waves in solid media, to present various heat maps to the students (heat maps in a lower frequency range, i.e., products k_0a lower than those used above, are, of course, also eligible to apply—see the Appendix). Finally, the main aim of the paper was to illustrate these abovementioned purposes by providing examples of heat maps, which can be used during lessons for (i) non-monochromatic plane waves in a fluid/isotropic solid interface, (ii) interaction of an acoustic beam with a fluid/solid interface (including anisotropic solid), and (iii) the same interaction (acoustic beam) when generalized Lamb waves and Rayleigh waves are generated.

APPENDIX: THE DECOMPOSITION INTO PLANE WAVES PRINCIPLE FOR A FLUID/FLUID STRUCTURE, AND ITS COMPUTATION

This appendix aims at explaining the decomposition into plane waves, which are principle in the basic case of the interaction of a bounded beam with an interface separating two fluid media, to help a reader to quite easily obtain heat maps similar to those given in this article. In particular, this appendix provides (i) the basic equations using spatial Fourier transforms, (ii) a method using matrix computation to calculate these Fourier transforms without using a fast Fourier transform (FFT) algorithm.

1. Incident field

The acoustic fields generated in a fluid labelled "0" by a finite-size emitter are acoustic beams, which are often called "bounded beams" just because the emitter has a finite size [see Fig. 10, in the case of a two-dimensional (2D) problem, invariant in the direction, y_e]. These types of bounded beams can be classically modeled as a continuous summation of monochromatic plane waves propagating in all

https://doi.org/10.1121/10.0013013

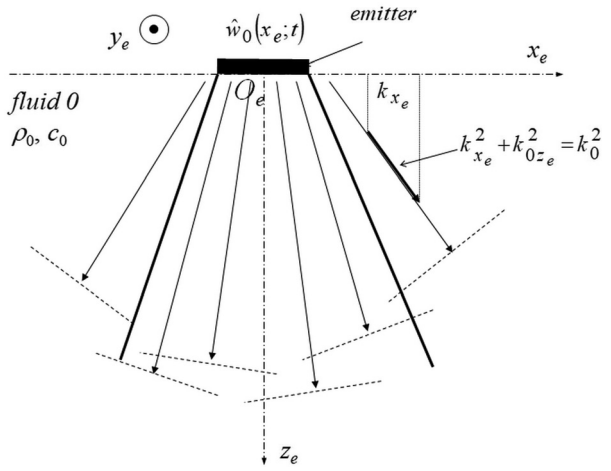

FIG. 10. Schematic diagram of the plane waves which constitute the acoustic bounded beam created by an emitter in a fluid medium.

directions of the half space (see Goodman.[4]) Each plane wave has its own amplitude, $\hat{A}_e(k_{x_e})$, and its own wavenumber vector, $\mathbf{k}_0 = \omega/c_0\,\mathbf{n}_e = k_{x_e}\,\mathbf{e}_{x_e} + k_{0z_e}\,\mathbf{e}_{z_e}$, where ω is the angular frequency of the waves. Note that the wave number, k_{0z_e}, may be complex (then, it is written as $\hat{k}_{0z}$) since the evanescent plane waves may be taken into account. $M(x_e, z_e)$ is any point of the half-space, $z_e > 0$, $\mathbf{n}_e$ is the propagation direction vector of the wave, c_0 is the propagation velocity of the wave, and $B_e = (\mathbf{e}_{x_e}, \mathbf{e}_{z_e})$ is the orthonormal basis associated with the coordinate system $R_e = (O_e, x_e, z_e)$.[4–13]

As a result of the linearity of the field equations, the complex incident acoustic pressure, $\hat{p}_{\text{inc}}(x_e, z_e; t) = \hat{P}_{\text{inc}}(x_e, z_e)\exp(-i\omega t)$, can, thus, be expressed as a superposition of a (theoretically) infinite number of plane waves, which takes the form of the following Fourier transform [omitting the $\exp(-i\omega t)$ factor][4] such that

$$\hat{P}_{\text{inc}}(x_e, z_e) = \int_{-\infty}^{+\infty} \hat{A}_e(k_{x_e}) \exp\left[\mathrm{i}\left(k_{x_e}x_e + \hat{k}_{0z_e}z_e\right)\right] dk_{x_e}, \quad \text{(A1)}$$

where $\hat{k}_{0z_e}$ is given by the following dispersion equation:

$$k_{x_e}^2 + \hat{k}_{0z_e}^2 = \|\,\mathbf{k}_0\,\| = k_0^2 = (\omega/c_0)^2, \quad \text{(A2)}$$

which is nothing but the necessary condition for the solution equation (A1) to satisfy the propagation equation. Due to the choice of the time factor, $\exp(-i\,\omega\,t)$, we must choose $\hat{k}_{0z_e}$ so that $\mathrm{Re}\{\hat{k}_{0z_e}\} \geq 0$ or $\mathrm{Im}\{\hat{k}_{0z_e}\} \geq 0$.

The normal displacement (or normal velocity, $\hat{w}_0$) of the front face of the emitting transducer can be given either experimentally or analytically. Assuming that the front face (assimilated, here, to a line of length, b) vibrates following its first mode, $W_0\cos(\pi x_e/b) \approx W_0\,[1 - (\pi x_e/b)^2]$, a Gaussian profile can be a good approximation of this velocity (which is, thus, assumed to be known),

$$\begin{aligned}\hat{w}_0(x_e;t) &= \hat{W}_0(x_e)\exp(-i\omega t)\\ &= W_0\exp\left(-x_e^2/a^2\right)\exp(-i\omega t),\end{aligned} \quad \text{(A3)}$$

where $a = b/\pi$ is the nominal radius of the emitter. Using the Euler equation,

$$\rho_0\partial\hat{\mathbf{w}}/\partial t + \nabla\hat{p} = \mathbf{0}, \quad \text{(A4)}$$

where ρ_0 is the density of the fluid, $\hat{\mathbf{w}}$ is the particle velocity vector, and the normal particle velocity, $\hat{w}_{z_e}$, in the fluid is given as a function of the acoustic pressure by

$$\begin{aligned}\hat{w}_{z_e}(x_e, z_e; t) &= k_{0z_e}/(\rho_0\omega)\hat{p}_{\text{inc}}(x_e, z_e; t)\\ &= \hat{W}_{z_e}(x_e, z_e)\exp(-i\omega t),\end{aligned} \quad \text{(A5)}$$

which, using Eq. (A1), leads to

$$\hat{W}_{z_e}(x_e, z_e = 0) = \frac{1}{\rho_0\omega}\int_{-\infty}^{+\infty} \hat{k}_{0z_e}\hat{A}_e(k_{x_e})\exp(\mathrm{i}k_{x_e}x_e)\,dk_{x_e}. \quad \text{(A6)}$$

Assuming that the normal velocity of the front face of the emitter and the normal particle velocity of the fluid are equal at $z_e = 0$, the amplitude of each plane wave can then be calculated by means of an inverse Fourier transform,

$$\hat{A}_e(k_{x_e}) = \frac{\rho_0\omega}{2\,\pi\,k_{0z_e}}\int_{-\infty}^{+\infty} \hat{W}_0(x_e)\exp(-\mathrm{i}k_{x_e}x_e)\,dx_e, \quad \text{(A7)}$$

and, therefore, since the amplitudes, $\hat{A}_e(k_{x_e})$, are known, the whole pressure field in fluid 0 can be calculated using the Fourier transform equation (A1), as it can be seen in Fig. 11.

2. The interaction of the incident field with a plane interface separating two fluid media

The study of the interaction of each plane wave with the interface separating fluid 0 from fluid 1 (celerity, c_1, and density, ρ_1) needs a change of coordinate system: a new coordinate system, $R = (O_e, x, z)$, linked to a –plane parallel to the interface and located at a distance, d, from it, is deduced from R_e by a rotation angle, θ, around y_e (incident angle of the acoustic beam, $O_e z_e$; see Fig. 12).

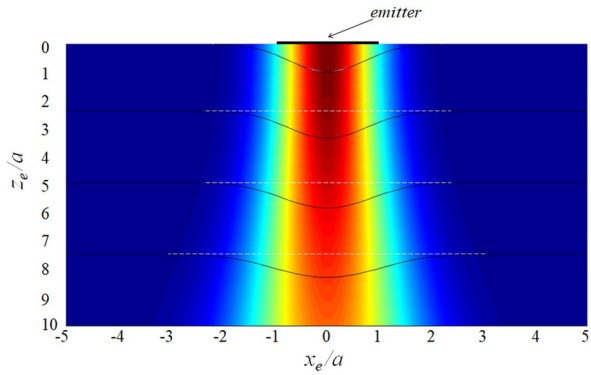

FIG. 11. (Color online) Cartography of the acoustic pressure field in a fluid (adimensional frequency, $k_0a = 15$) with four cuts at $z_e = 0$, $z_e = 2.5a$, $z_e = 5a$, and $z_e = 7.5a$.

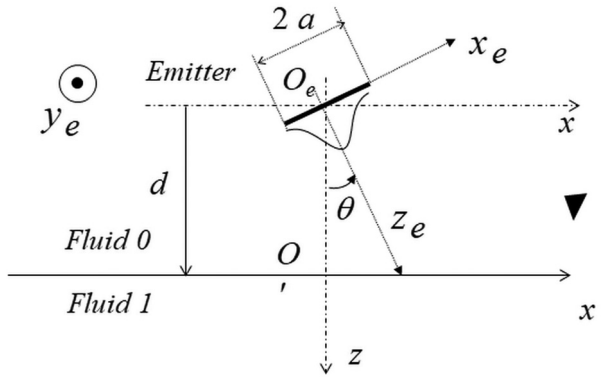

FIG. 12. Geometry of the problem for a plane interface separating two fluid media.

The coordinates of a given point, M, in this new coordinate system are denoted by $M(x,z)$, and the components of each wave vector, $\mathbf{k}_0$, are denoted by $(k_x, \hat{k}_{0z})$. These components depend on k_{x_e} through the dispersion equation (A2) and the following equations:

$$k_x = k_{x_e}\cos\theta + \hat{k}_{0z_e}\sin\theta, \tag{A8a}$$

$$\hat{k}_{0z} = -k_{x_e}\sin\theta + \hat{k}_{0z_e}\cos\theta. \tag{A8b}$$

It should be noted that the invariance of the dot product,

$$\mathbf{k}_0 \cdot \mathbf{O}_e\mathbf{M} = k_{x_e}x_e + \hat{k}_{0z_e}z_e = k_x x + \hat{k}_{0z}z, \tag{A9}$$

leads to the following expression for the incident acoustic pressure, $\hat{P}_{\text{inc}}$, in the fluid 0 in the coordinate system, R, such that

$$\hat{P}_{\text{inc}}(x,z) = \int_{-\infty}^{+\infty} \hat{A}'_e(k_{x_e})\exp\left[\mathrm{i}\hat{k}_{0z}(z-d)\right]\exp\left(\mathrm{i}k_x x\right)dk_{x_e}, \tag{A10}$$

where

$$\hat{A}'_e(k_{x_e}) = \hat{A}_e(k_{x_e})\exp\left(\mathrm{i}\hat{k}_{0z}d\right). \tag{A11}$$

Note that the amplitudes $\hat{A}_e(k_{x_e})$ and $\hat{A}'_e(k_{x_e})$ are, respectively, referenced at points O_e and O' (see Fig. 12).

When interacting with the interface, each incident plane wave of amplitude $\hat{A}'_e(k_{x_e})$ and wave vector $\mathbf{k}_0(k_{x_e})$ propagating in fluid 0 will generate a reflected wave in fluid 0 with wave vector $\mathbf{k}'_0(k_{x_e})$ and a transmitted wave in fluid 1 with wave vector $\mathbf{k}_1(k_{x_e})$. These three wave vectors have the same projections on the interface, namely,

$$\mathbf{k}_0 \cdot \mathbf{e}_x = \mathbf{k}'_0 \cdot \mathbf{e}_x = \mathbf{k}_1 \cdot \mathbf{e}_x = k_x(k_{x_e}), \tag{A12}$$

which leads to the well-known Snell-Descartes law. Note that the wave number $k_{1z} = \mathbf{k}_1 \cdot \mathbf{e}_z$ must be chosen carefully to ensure the correct behavior of the transmitted waves at infinity (see, for example, Ref. 13, Chap. 12, exercise 1.2.1, p. 151).

Then, the reflection and transmission coefficients (for the pressure) are classically given by[1–3]

$$\hat{R} = \frac{\rho_1\hat{k}_{0z} - \rho_0\hat{k}_{1z}}{\rho_1\hat{k}_{0z} + \rho_0\hat{k}_{1z}} \tag{A13a}$$

and

$$\hat{T} = \frac{2\rho_1\hat{k}_{0z}}{\rho_1\hat{k}_{0z} + \rho_0\hat{k}_{1z}}, \tag{A13b}$$

where the "carets" recall that the corresponding variables can take complex values.

The reflected and transmitted fields in fluids 0 and 1 can then be reconstructed, leading to the following Fourier transformations:

$$\hat{P}_{\text{ref}}(x,z) = \int_{-\infty}^{+\infty} \hat{R}(k_x)\hat{A}'_e(k_{x_e})\exp\left\{\mathrm{i}\left[k_x x - \hat{k}_{0z}(z-d)\right]\right\}dk_{x_e} \tag{A14a}$$

and

$$\hat{P}_{\text{tr}}(x,z) = \int_{-\infty}^{+\infty} \hat{T}(k_x)\hat{A}'_e(k_{x_e})\exp\left\{\mathrm{i}\left[k_x x + \hat{k}_{1z}(z-d)\right]\right\}dk_{x_e}. \tag{A14b}$$

3. Calculation of Fourier transforms

The Fourier integrals (A1) and (A14) have the following form:

$$I(x,z) = \int_{-\infty}^{+\infty} \hat{F}(k_{x_e})\exp\left\{\mathrm{i}\left(k_x x + \hat{k}_z z\right)\right\}dk_{x_e}, \tag{A15}$$

where k_x and $\hat{k}_z$ are functions of k_{x_e}. It is worthwhile to note that the integration variable, k_{x_e}, and the space coordinate, x, are no longer Fourier conjugate variables due to the rotation of the coordinate axes. So, the FFT algorithm is inappropriate. To calculate the integral (A15), we use a simple classical trapezoidal method on the basis of the initial sampling used for k_{x_e} [and using the invariance (A9) of the dot product, $\mathbf{k}_0 \cdot \mathbf{O}_e\mathbf{M}$, abovementioned]. The advantage of this method is to easily show the acoustic fields in the different media either in the form of heat maps linked to the structure [i.e., linked to the coordinate system (Oxz)] or through cuts of the acoustic fields in a plane parallel to the structure (thus, at a given z). Moreover, due to the factorization properties of the exponential function, a matrix computation using, for example, MATLAB® or SCILAB software, permits us to calculate all of the Fourier integrals in a single step. The procedure is the following.

Using the properties of the exponential function, integral (A15) is first written as

$$I(x,z) = \int_{-\infty}^{+\infty} \exp\left(\mathrm{i}\hat{k}_z z\right)\hat{F}(k_{x_e})\exp\left(\mathrm{i}k_x x\right)dk_{x_e}. \tag{A16}$$

https://doi.org/10.1121/10.0013013

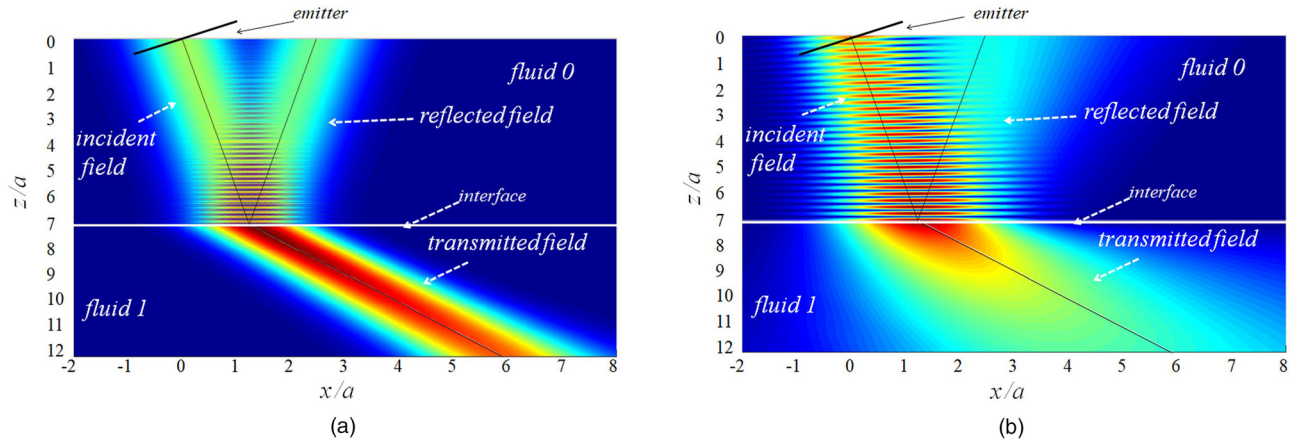

FIG. 13. (Color online) Heat maps of the modulus of the acoustic pressure for a fluid 0/fluid 1 structure. $c_0 = 1480\ \mathrm{m\,s^{-1}}$, $\rho_0 = 1000\ \mathrm{kg\ m^{-3}}$, $c_1 = 5825\ \mathrm{m\,s^{-1}}$, $\rho_1 = 5000\ \mathrm{kg\ m^{-3}}$, $a = 10$ mm, and $\theta = 10°$. The oblique lines correspond to the incident, reflected, and transmitted rays, such as was predicted by Snell-Descartes law (A12). (a) $f = 2$ MHz ($k_0 a = 84.9$) and (b) $f = 0.3$ MHz ($k_0 a = 12.7$).

In the case of the Gaussian beam (A3), the integration domain may be reduced to a segment $[-k_0 + \varepsilon, k_0 - \varepsilon]$ in such a way that the singular points are outside of the domain.

For a sampling of the different variables x, z, and k_{x_e}, leading to, respectively, N_x, N_z, and $N_{k_{x_e}}$ values, three matrices are built such that

(i) a $(N_z \times N_{k_{x_e}})$ matrix corresponding to the term $\exp\left(\mathrm{i}\,\hat{k}_z z\right)$,
(ii) a $(N_{k_{x_e}} \times N_x)$ matrix corresponding to the term $\hat{F}\left(k_{x_e}\right)$ (column of $N_{k_{x_e}}$ values replicated N_x times to have N_x identical columns, where the first and the last row are divided by two), and
(iii) a $(N_{k_{x_e}} \times N_x)$ matrix corresponding to the term $\exp\left(\mathrm{i}k_x x\right)$.

As the trapezoidal method consists in calculating the integral of the function $f(x)$ over the interval $[a, b]$, using the following summation [here, for a constant step sampling of $(n+1)$ values x_i]

$$\int_a^b f(x)\,dx = \lim_{n\to+\infty}\left[\frac{f(a)}{2} + \sum_{i=1}^{n-1} f(x_i) + \frac{f(b)}{2}\right], \qquad \text{(A17)}$$

where $\Delta x = (b-a)/n$, $x_0 = a$, and $x_i = x_{i-1} + \Delta x$, it is easy to see that the integral (A16) can be calculated using matrix products, which can be symbolically written as

$$\left[\exp\left(\mathrm{i}\,\hat{k}_z z\right)\right] * \left[\hat{F}(k_{x_e})\exp\left(\mathrm{i}k_x x\right)\right]\,\Delta k_{x_e}, \qquad \text{(A18)}$$

where the matrices in the second set of brackets are multiplied term by term and Δk_{x_e} is the step of the sampling for k_{x_e}. The MATLAB® or SCILAB (for instance) code could be written as

```
kxemin = -0.9 * k0;
kxemax = 0.9 * k0;
Nx = length(x); % number of points for x
Nz = length(z); % number of points for z
Nkxe = length(kxe); % number of points for kxe
dkxe = kxe(2) - kxe(1); % step sampling for kxe
F(1) = F(1)/2; % 1st term corresponding to f(a)/2
F(Nkxe) = F(Nkxe)/2; % last term corresponding to f(b)/2
FF = repmat(F.', [1 Nx]); % replication of Nx columns
TF = exp(i*z.'*kz) * (FF .* exp(i*kx.' * x)) * dkxe;
```

4. Application to heat maps of acoustic fields

Using the above-described method, heat maps of the acoustic pressure in fluids 0 and 1 can, thus, be drawn. The heat maps of Figs. 13(a) and 13(b) show the incident, reflected, and transmitted fields. In the higher frequency range [$k_0 a = 212$; Fig. 13(a)], the beams are narrow and follow, well, the oblique lines corresponding to Snell-Descartes law (A12). Moreover, the total field in fluid 0 highlights the interferences between the incident and the reflected fields. In the lower frequency range [$k_0 a = 12.7$, Fig. 13(b)], the beams are wider and do not follow the Snell-Descartes law as well as in the higher frequency range.

[1]B. A. Auld, *Acoustic Fields and Waves in Solids* (Wiley, New York, 1973).
[2]J. L. Rose, *Ultrasonic Waves in Solid Media* (Cambridge University Press, Cambridge, UK, 1999).
[3]D. Royer and E. Dieulesaint, *Elastic Waves in Solids I: Free and Guided Propagation* (Springer, Berlin, 2000).
[4]J. W. Goodman, *Introduction to Fourier Optics*, 4th ed. (Freeman, San Francisco, 2017).
[5]J. Pott and J. G. Harris, "Scattering of an acoustic Gaussian beam from a fluid–solid interface," J. Acoust. Soc. Am. **76**(6), 1829–1837 (1984).
[6]B. Hosten and M. Deschamps, "Transmission ultrasonore en faisceau borné d'une interface plane à l'aide du spectre angulaire d'ondes planes" ("Ultrasonic transmission of a bounded beam through a plane interface, using plane wave angular spectrum method"), Traitement du Signal **2**, 195–199 (1985).

[7]M. Rousseau and Ph. Gatignol, "Theory of the acoustic bounded beam," in *Acoustic Interactions with Submerged Elastic Structures, Part I*, Series on Stability, Vibration and Control of Systems Series B, edited by A. Guran, J. Ripoche, and F. Ziegler (World Scientific, Singapore, 1996), Vol. 5, pp. 207–241.
[8]D. Orofino and P. Pedersen, "Efficient angular spectrum decomposition of acoustic source—Part I: Theory," IEEE Trans. Ultrason., Ferroelect., Freq. Contr. **40**(3), 238–249 (1993).
[9]C. Potel, S. Baly, J. F. de Belleval, M. Lowe, and Ph. Gatignol, "Deviation of a monochromatic Lamb wave beam in anisotropic multilayered media: Asymptotic analysis, numerical and experimental results," IEEE Trans. Ultrason., Ferroelect., Freq. Contr. **52**(6), 987–1001 (2005).
[10]M. E. Schafer, P. A. Lewin, and J. M. Reid, "Propagation through inhomogeneous media using the angular spectrum method," in *Proceedings of the IEEE Ultrasonics Symposium*, 1987 pp. 943–945
[11]M. E. Schafer and P. A. Lewin, "Transducer characterization using the angular spectrum method," J. Acoust. Soc. Am. **85**, 2204–2214 (1989).
[12]C. Potel, Ph. Gatignol, and J. F. de Belleval, "Deviation of the modal waves excited by an ultrasonic monochromatic beam in an anisotropic layer," C. R. Acad. Sci. Paris, Série IIb Mech. **329**(11), 815–822 (2001).
[13]M. Bruneau, Ph. Gatignol, P. Lanceleur, and C. Potel, "Exercices d'acoustique—Corrigés détaillés. Rappels de cours" ("Exercices of acoustics—Detailed solutions. Course reminders") (Cépaduès Editions, Toulouse, France, 2021), Problèmes avancés (Advanced Exercises), Vol. 3.
[14]S. I. Rokhlin, T. K. Bolland, and A. Adler, "Reflection and refraction of elastic waves on a plane interface between two generally anisotropic media," J. Acoust. Soc. Am. **79**(4), 906–918 (1986).
[15]W. D. Hayes, "Conservation of action and modal wave action," Proc. R. Soc. London A. **320**, 187–208 (1970), available at https://www.jstor.org/stable/77799.
[16]D. E. Chimenti and A. H. Nayfeh, "Leaky Lamb waves in fibrous composite laminates," J. Appl. Phys. **58**(12), 4531–4538 (1985).